



**HAL**  
open science

# Guanine Tautomerism in Ionic Complexes with Ag + Investigated by IRMPD Spectroscopy and Mass Spectrometry

Andrés Cruz-Ortiz, Franco Molina, Philippe Maitre, Gustavo Pino

► **To cite this version:**

Andrés Cruz-Ortiz, Franco Molina, Philippe Maitre, Gustavo Pino. Guanine Tautomerism in Ionic Complexes with Ag + Investigated by IRMPD Spectroscopy and Mass Spectrometry. *Journal of Physical Chemistry B*, 2021, 125 (26), pp.7137-7146. 10.1021/acs.jpccb.1c03796 . hal-03324677

**HAL Id: hal-03324677**

**<https://hal.science/hal-03324677>**

Submitted on 23 Aug 2021

**HAL** is a multi-disciplinary open access archive for the deposit and dissemination of scientific research documents, whether they are published or not. The documents may come from teaching and research institutions in France or abroad, or from public or private research centers.

L'archive ouverte pluridisciplinaire **HAL**, est destinée au dépôt et à la diffusion de documents scientifiques de niveau recherche, publiés ou non, émanant des établissements d'enseignement et de recherche français ou étrangers, des laboratoires publics ou privés.

# **“Guanine Tautomerism in Ionic Complexes with Ag<sup>+</sup> Investigated by IRMPD Spectroscopy and Mass Spectrometry”**

Andrés F. Cruz-Ortiz, Franco L. Molina, Philippe Maitre and Gustavo A. Pino\*

<sup>a</sup> INFIQC (CONICET-UNC), Ciudad Universitaria, Pabellón Argentina, 5000 Córdoba, Argentina.

<sup>b</sup> Departamento de Fisicoquímica, Fac. de Ciencias Químicas, Universidad Nacional de Córdoba, Ciudad Universitaria, Pabellón Argentina, X5000HUA Córdoba, Argentina.

<sup>c</sup> Centro Láser de Ciencias Moleculares, Universidad Nacional de Córdoba, Ciudad Universitaria, Pabellón Argentina, X5000HUA Córdoba, Argentina.

<sup>d</sup> Université Paris-Saclay, CNRS, Institut de Chimie Physique, 91405, Orsay, France.

\*Corresponding author: [gpino@unc.edu.ar](mailto:gpino@unc.edu.ar)

## Abstract

In this paper we present the IRMPD spectra of three ionic complexes between guanine (G) and silver ( $\text{Ag}^+$ ):  $[\text{GAg-H}_2\text{O}]^+$ ,  $[\text{GAgG}]^+$  produced in the Electrospray Ionization Source of the mass-spectrometer and  $[\text{GAg}]^+$  produced by Collision Induced Dissociation of the  $[\text{GAgG}]^+$  complex. Based on comparison of theoretically calculated IR spectra, we show that there are two isomers of each complex containing two different keto-amino (KA) tautomers of G (GKA(1,9) and GKA(1,7)). The observed isomers are the most stable structures in aqueous solution and their experimentally estimated relative populations are in better agreement with the calculated relative populations in solution than in gas phase, both at 298 K. We concluded that these observations suggest that GKA(1,9) and GKA(1,7) co-exist in solution according to previous theoretical reports (Colominas, C.; et al. *J. Am. Chem. Soc.* **1996**, *118*, 6811). We were unable to find any evidence of the presence of the GEA(9), GKA(3,7), GKA(3,9) or GKA(7,9), whose relative stabilities in solution are strongly dependent on the theoretical method used to account for the solvent effect (Hanus, M.; et al. *J. Am. Chem. Soc.* **2003**, *125*, 7678).

## 1. Introduction

The five nucleic acid bases cytosine (C), thymine (T), Uracil (U), adenine (A) and guanine (G) are of fundamental importance in biology, being the building blocks for the genetic code.<sup>1</sup> In the canonical structure of the nucleic acids they form specific pairs G-C and A-T in DNA, while T is replaced by U to form A-U pair in RNA. The recognition of the G-C pair takes place through three intermolecular H-bonds while in the case of A-T and A-U the recognition involves two intermolecular H-bonds.<sup>1</sup>

The five bases exist in several tautomeric forms, but only one tautomer of each one is considered a canonical structure for the specific recognition and genetic information transfer. If a rare tautomer is introduced in DNA or RNA, the H-bonding pattern changes and as a consequence the failed recognition leads to a point mutation.<sup>2</sup>

In this sense, characterizing the structure of the tautomers of the five bases and their relative stability in different environments has been of great interest for a long time. In recent years, relentless efforts have been focused on the study of isolated neutral bases in gas phase so that detailed comparisons between theory and experiment can be made. Readers are referred to Ref. 3 and 4 for a review of all these works.

Guanine is the nucleobase with the largest number of tautomeric forms (keto, enol, amino, imino, N1H-N3H, N7H-N9H). In this regard, there have been several studies devoted to characterize the different tautomers of G that co-exist in the gas phase, including REMPI (IR-UV hole burning) spectroscopy,<sup>5-12</sup> IR laser spectroscopy in He-nanodroplets,<sup>13</sup> Fourier transform microwave (FTMW) spectroscopy in a molecular beam.<sup>14</sup> Although several discrepancies were found between the different reports, it was finally concluded that in gas phase the most populated isomers of G are the two keto-amino tautomers, GKA(1,9) and GKA(1,7) and two rotamers of the enol-amino tautomer GEA(9),<sup>3,4</sup> shown in Scheme 1 together with the calculated relative stabilities in gas and aqueous phase.<sup>15</sup> The numbers in parenthesis indicate the N heteroatoms to which the H atoms are bonded.

It must be notice that the GKA(1,9), GKA(1,7) and GEA(9)<sub>anti</sub> were not detected by REMPI, due to their short (sub-picosecond) excited state lifetime, but their presence as major tautomers was confirmed by the most recent works on He-nanodroplets IR spectroscopy<sup>13</sup> and FTMW spectroscopy<sup>14</sup>.

In aqueous solution, the keto-amino forms are expected to dominate. However, studies on the structure and stability of G tautomers in solution are mainly based on theoretical predictions.<sup>16</sup> In the seminal work of Colominas et al.<sup>17</sup> the authors calculated

the relative Gibbs hydration energies of the five lowest energy tautomers of G in gas phase, using the optimized versions of the continuum model developed by Miertus, Scrocco, and Tomasi (MST)<sup>18,19</sup> as well as the Monte Carlo free energy perturbation (MC-FEP) techniques.<sup>20</sup> From these calculations, it was concluded that only the GKA(1,9) and GKA(1,7) tautomers could co-exist in aqueous solution in which they are almost isoenergetic within 1-2 kcal/mol depending on the calculation method.

More recently, M. Hanus et al.<sup>15</sup> extended the study to the other more energetic tautomers in gas phase and performed a similar calculation using the continuum solvation model CONductor-like Screening MOdel (COSMO) and the Molecular Dynamics-Thermodynamic Integration (MD-TI) technique to calculate the relative Gibbs energy of hydration between different G tautomers. The results from the COSMO method are in agreement with those of Ref. 17, finding GKA(1,9) and GKA(1,7) as the most stable structures in aqueous solution. However, the MD-TI calculations suggest that the GKA(3,7), GKA(7,9) and GKA(3,9) tautomers are ~ 7–13 kcal/mol more stable than the GKA(1,9) and GKA(1,7) tautomers in aqueous phase.

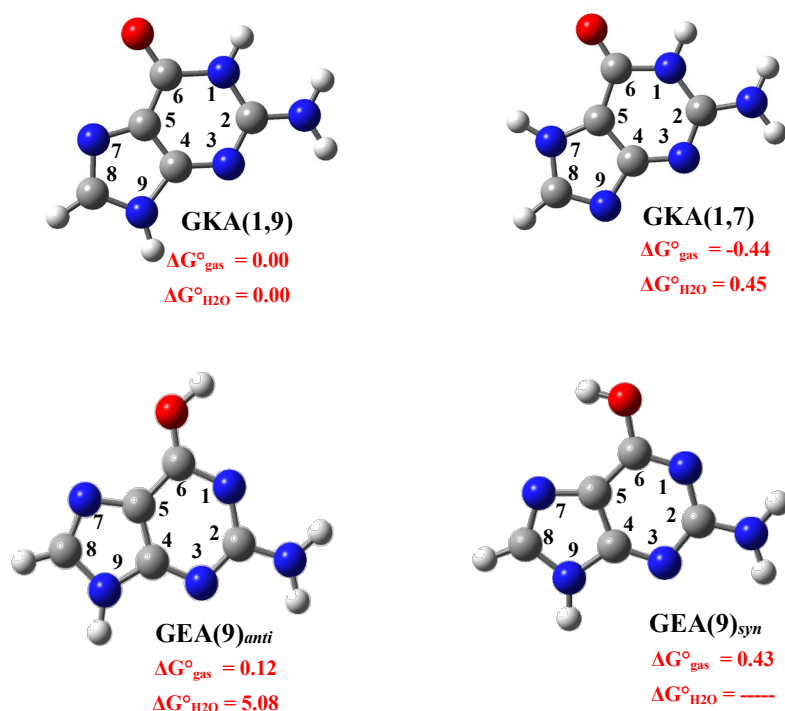
In solution, cationizing agents may bind to bases, and thereby favor alternative tautomers. As a consequence, the specific H-bonding pattern between complementary bases is lost. Effects of protonation and metal cations attachments have been studied in gas phase. The structure of protonated G ( $\text{GH}^+$ ) in gas phase has been characterized by cold ions UV-fragmentation spectroscopy.<sup>21</sup> Under these experimental conditions only one tautomer ( $\text{GKA}(1,7,9)\text{H}^+$ ) was observed that could be produced either from the protonation of neutral GKA(1,9) on N7 or from the protonation of neutral GKA(1,7) on N9. The use of a different cation instead of  $\text{H}^+$  could help to distinguish the tautomeric form of neutral G interacting with the cation.

In this sense, there are few recent studies on the interaction of G with several metal cation ( $\text{M}^+$ ).<sup>22-29</sup> However, the electronic nature of these cations could lead to very different interaction motif as compared to  $\text{H}^+$ . More recently, we characterized two isomers of the silver mediated  $[\text{GCAg}]^+$  pair, one of them containing GKA(1,9) and the other one with GKA(1,7).<sup>30</sup>

In this sense, the interaction of C with different cations<sup>31-34</sup> has been extensively studied and it was recently shown that  $\text{Ag}^+$  leads the same interaction motif as  $\text{H}^+$ .<sup>30,35-37</sup>

Therefore,  $\text{Ag}^+$  is a candidate to study its interaction with G to compare with  $\text{GH}^+$ . As a consequence in this work we present the results of interaction of G with  $\text{Ag}^+$  in the  $[\text{GAg-H}_2\text{O}]^+$  and  $[\text{GAgG}]^+$  complexes produced in an electrospray ionization source

(ESI) from an aqueous solution and in the  $[\text{GAg}]^+$  complex produced from collision induced dissociation (CID) of the  $[\text{GAgG}]^+$  complex in the gas phase.



**Scheme 1.** Structure and numbering of the most stable tautomers of Guanine. The numbers in parentheses indicate the position of the H that determines the tautomeric form.  $\Delta G^\circ$  values at 298 K are taken from the reference 15 and expressed in kcal/mol. The reported value of  $\Delta G^\circ_{\text{H}_2\text{O}}$  from reference 15 were calculated using the continuum solvation model COSMO.

## 2. Experimental and computational methods

### 2.1 IRMPD spectroscopy

All reagents (from sigma Aldrich) were used without further purification. The  $[\text{GAg-H}_2\text{O}]^+$  and  $[\text{GAgG}]^+$  complexes were generated in an electrospray ionization source (ESI) from a solution containing 300  $\mu\text{M}$  of  $\text{AgNO}_3$  and 370  $\mu\text{M}$  of Guanine (G) in a methanol:water = 1:1 mixture as a solvent. The ions generated were analyzed and mass selected in a hybrid mass spectrometer FT-ICR (7T FT-ICR Bruker Apex Qe).<sup>38</sup> The ionic complex were isolated in the quadrupole interface of the mass spectrometer and then transferred to the hexapolar trap, where they were accumulated and thermalized.<sup>38,39</sup> Finally, the selected and thermalized ions were transferred to the ICR cell where they were probed by Infrared Multiphoton Dissociation (IRMPD) spectroscopy.

The IRMPD spectra of the complexes were obtained in the spectral range 1250–1850  $\text{cm}^{-1}$  with the tunable IR radiation from the Free Electron Laser (IR-FEL),<sup>40</sup> and the  $\text{CO}_2$  laser available at CLIO,<sup>41</sup> coupled to the FT-ICR mass spectrometer. By

monitoring the intensities of precursor ( $I_p$ ) and resulting fragment ions ( $I_{frag}$ ) as a function of the laser frequency, the IRMPD spectrum was obtained as the fragmentation efficiency ( $eff$ ) according to equation 1.

$$eff(h\nu) = -Ln\left(\frac{I_p(h\nu)}{[I_p(h\nu) + \sum I_{frag}(h\nu)]}\right) \quad (1)$$

The  $[GAg]^+$  complex was produced by Collision Induced Dissociation (CID) of the  $[GAgG]^+$  complex in the 3.2 section, as will be explained in section 3.3.

## 2.2 Computational details

Electronic structure calculations for the possible isomers of the  $[GAg-H_2O]^+$ ,  $[GAgG]^+$  and  $[GAg]^+$  complexes in the gas phase were performed with Gaussian 09 Revision E.01<sup>42</sup> at the density functional theory (DFT) level. The geometry optimization and frequencies calculations were carried out with the correlation and exchange hybrid functional B3LYP<sup>43,44</sup> employing the 6-311G++ (d,p) basis set for the C, H, O, and N atoms, and the Stuttgart-Dresden (SSD) effective core pseudo-potential basis set for Ag<sup>45</sup> in gas and solution phase, without symmetry constraints. The zero point energies (ZPEs) for all complexes were determined using the vibrational frequencies calculated in each phase. The values of  $\Delta G^\circ$  were also calculated with the spectroscopic constant obtained in each phase and using the rigid rotor harmonic oscillator approximation (RRHO).

The ability of B3LYP with several basis set for the determination of molecular properties of DNA bases and other small aromatic molecules has been extensively tested.<sup>46,47</sup> In particular, the combination of B3LYP/6-311G++ (d,p) with SSD effective core pseudo-potential basis set for Ag has shown to be suitable for predicting the structure and vibrational frequencies of several ionic complexes between DNA bases and Ag<sup>+</sup>.<sup>30,33,35</sup>

In order to validate the relative energies obtained at the DFT level, single point energy refinement at the CCD/6-311++G(d,p)// B3LYP/6-311G++ (d,p) level of theory was also performed for the most stable isomers of  $[GAg-H_2O]^+$ .

The relative Gibbs energies at 298 K were also calculated. This temperature compares that established for multiple collisions with Ar in the hexapolar ion trap of the hybrid mass spectrometer 7T FT-ICR.<sup>38,39</sup>

Calculated vibrational frequencies were scaled by a factor 0.983, as considered the most appropriate scaling factor value for the theory level used.<sup>48</sup> For a better comparison with the IRMPD spectra, each calculated IR band was convolved by a Gaussian profile assuming a bandwidth of 15 cm<sup>-1</sup> at the full width half maximum (FWHM) which is typically the spectral bandwidth IR-FEL in the spectral region (1250–1850 cm<sup>-1</sup>).

Finally, the effect of the solvent on the relative stability and structure of the different isomers was calculated at the same theory level using the polarizable continuum model (PCM) assuming water as solvent.<sup>49</sup> Some comparisons with the integral equation formalisms (IFPCM) implemented in Gaussian09 was also performed for the for the most stables isomers of [GAg–H<sub>2</sub>O]<sup>+</sup>. A very good agreement between IFPCM and COSMO has been reported for a large sets of ionic and neutral species.<sup>50</sup>

### 3. Results and discussion

The [GAg–H<sub>2</sub>O]<sup>+</sup> and [GAgG]<sup>+</sup> complexes were produced in the ESI source as the main species containing G and Ag<sup>+</sup>. However, [GAg]<sup>+</sup> could not be observed in the mass spectrum, although several experimental conditions were used. Therefore, in the following paragraph we present the IRMPD spectroscopy of the two former complexes.

#### 3.1. [GAg–H<sub>2</sub>O]<sup>+</sup> complex

The fragmentation of the [GAg–H<sub>2</sub>O]<sup>+</sup> complex after irradiation with IR-FEL photons during 500 ms leads only to the loss of the neutral water molecule. This fragmentation channel has been previously observed by IRMPD for the related [CAG–H<sub>2</sub>O]<sup>+</sup> complex.<sup>33</sup> The IRMPD spectrum of the [GAg–H<sub>2</sub>O]<sup>+</sup> complex is shown in Figure 1a.

As mentioned in the introduction section, three tautomeric structures of neutral G have been previously found in the gas phase, GKA(1,9), GKA(1,7) and GEA(9) (scheme 1),<sup>3,4</sup> while in aqueous solution, GKA(1,9) and GKA(1,7) or GKA(3,7), GKA(3,9) and GKA(7,9) are suggested to be the stable tautomers, depending on the method used to calculate the hydration effect.<sup>15,17</sup> In this regard we have calculated different structures of the [GAg–H<sub>2</sub>O]<sup>+</sup> complex considering the GKA(1,9), GKA(1,7), GEA(9), GKA(3,7), GKA(3,9), GKA(7,9) tautomers of G as well as GEA(7). Several local minima were found and the four lowest energy structures are displayed in Table 1, while a complete list of the different isomers studied in this work is presented in Tables SI 1-6 and Figures SI 1-6 (Supplementary Information).



A good agreement is observed in Table 1 between  $\Delta G^{\circ}_{298K}$  for the most stable isomers of the  $[\text{GAg-H}_2\text{O}]^+$  complex in gas phase calculated at B3LYP and CCD//B3LYP levels, which allows validating the use of B3LYP only for the other systems studied in this work.

For comparison, the solvation effect in this complex was accounted for considering the PCM and IFPCM methods which is known to lead to similar results to those of COSMO model.<sup>50</sup> In Table 1, a good agreement is also observed between PCM and IFPCM results. Then, the PCM method is used in all other complexes studied in this work.

The most stable and populated isomers, either in the gas and solution phase are the two GKA(1,9) and GKA(1,7) tautomers, interacting with  $\text{Ag}^+$  on N7 and N9, respectively, in line with previous studies on the interaction of G with monovalent cations.<sup>24-27,51</sup> This is also in agreement with our previous results on  $[\text{GCAg}]^+$  complex for which two isomers were found: one of them containing GKA(1,9) and the other one containing GKA(1,7).<sup>30</sup>

The  $\text{H}_2\text{O}$  molecule in the  $[\text{GAg-H}_2\text{O}]^+$  complex preferentially binds to  $\text{Ag}^+$  leading to a linear di-coordinated complex of the metal cation as previously observed for the  $[\text{CAg-H}_2\text{O}]^+$  complex.<sup>33</sup> The interaction of  $\text{H}_2\text{O}$  with different sites of G resulted complexes that are 8-14 kcal/mol less stable than those with  $\text{H}_2\text{O}$  interacting with  $\text{Ag}^+$  as shown in Tables SI 7 and 8 for GKA(1,9) and GKA(1,7), respectively.

In the gas phase, the first local minimum  $[\text{GKA}(1,7)\text{N9Ag-H}_2\text{O}]^+$  lies 4.0 kcal/mol above the global minimum  $[\text{GKA}(1,9)\text{N7Ag-H}_2\text{O}]^+$ , while when the solvent effect is implicitly considered this difference is only 0.3 kcal/mol. In the second local minimum  $[\text{GEA}(9)_{\text{anti}}\text{N7Ag-H}_2\text{O}]^+$  the interaction between  $\text{GEA}(9)_{\text{anti}}$  and  $\text{Ag}^+$  occurs through N7. This isomer is found 6.7 kcal/mol and 6.9 kcal/mol above the global minimum in the gas and aqueous phase, respectively. Finally, the interaction between the N3 of GKA(1,7) and  $\text{Ag}^+$  is less favorable in the gas phase (7.9 kcal/mol). However, when the solvent effect is considered, this isomer is significantly stabilized and it is found at only 2.4 kcal/mol above the global minimum, which suggests that the formation of this isomer in the solution cannot be ruled out.

The preferential stabilization in gas phase of the canonical tautomer GKA(1,9) over GKA(1,7) upon interaction with  $\text{Ag}^+$  is evident from the comparison of the relative stability reported for the complexes in Table 1 with the relative stability of the bare tautomers shown in Scheme 1.<sup>15</sup>

The structural assignment of the  $[\text{GAg-H}_2\text{O}]^+$  complex was based on the comparison of the IRMPD spectrum with linear IR absorption spectra calculated for the most stable isomers, shown in Fig. 1 (b-d).



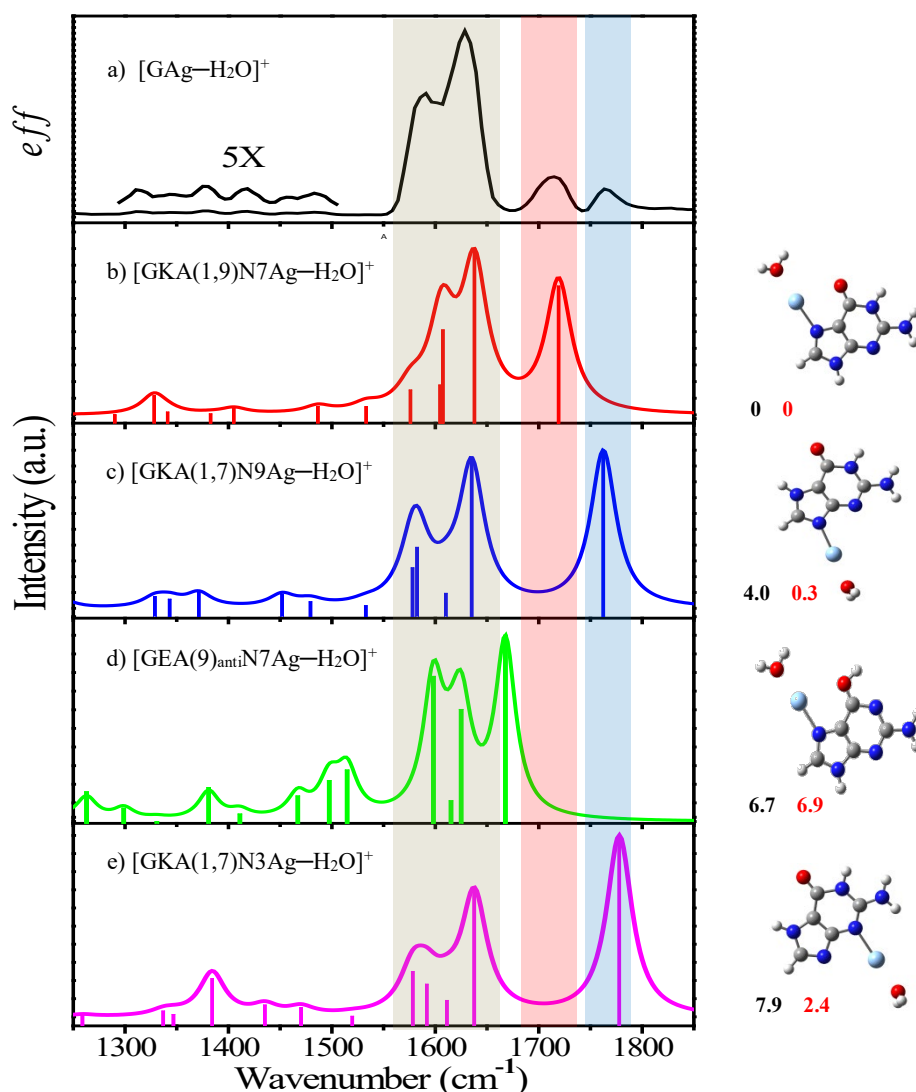


**Figure 1.** a) Experimental IRMPD spectrum of  $[\text{GAg-H}_2\text{O}]^+$  complex recorded in the spectral range  $1250\text{--}1850\text{ cm}^{-1}$  and calculated spectra of the four lowest energy isomers calculated at the B3LYP/6-311G++(d,p) and SDD level for  $\text{Ag}^+$ : b)  $[\text{GKA}(1,9)\text{N7Ag-H}_2\text{O}]^+$ , c)  $[\text{GKA}(1,7)\text{N9Ag-H}_2\text{O}]^+$ , d)  $[\text{GEA}(9)_{\text{anti}}\text{N7Ag-H}_2\text{O}]^+$  and e)  $[\text{GKA}(1,7)\text{N3Ag-H}_2\text{O}]^+$ . The vibrational frequencies were corrected with a factor of 0.983. The relative standard Gibbs energies in gas (black numbers) and solution (red numbers) phase are reported in kcal/mol.

In the IRMPD spectrum (Fig. 1a) three well-defined spectral features are observed at  $1765\text{ cm}^{-1}$ ,  $1715\text{ cm}^{-1}$  and in the  $1550\text{--}1650\text{ cm}^{-1}$  region. The linear IR absorption spectra calculated for the  $[\text{GKA}(1,9)\text{N7Ag-H}_2\text{O}]^+$  isomer is in good agreement with the IRMPD spectrum. However, the experimental band at  $1764\text{ cm}^{-1}$  cannot be assigned considering only the global minimum, thus the contribution of other isomers needs to be considered.

Particularly remarkable are the transitions observed in the  $1700\text{--}1800\text{ cm}^{-1}$  region where the C=O stretching modes are expected. The band observed at  $1715\text{ cm}^{-1}$  in the

IRMPD spectrum is assigned to the C=O stretch mode of GKA(1,9) calculated at 1719  $\text{cm}^{-1}$  for the  $[\text{GKA}(1,9)\text{N7Ag-H}_2\text{O}]^+$  isomer. The band observed at 1765  $\text{cm}^{-1}$  in the IRMPD spectrum can be assigned to the C=O stretching mode of GKA(1,7) calculated at 1763 and 1777  $\text{cm}^{-1}$  in  $[\text{GKA}(1,7)\text{N9Ag-H}_2\text{O}]^+$  and  $[\text{GKA}(1,7)\text{N3Ag-H}_2\text{O}]^+$  isomers, respectively. Considering the predicted relative population of these two isomers in the gas and aqueous phases, it is reasonable to assign the band at 1765  $\text{cm}^{-1}$  to the  $[\text{GKA}(1,7)\text{N9Ag-H}_2\text{O}]^+$  isomer.

The presence of the  $[\text{GEA}(9)_{\text{anti}}\text{N7Ag-H}_2\text{O}]^+$  isomer is neglected based on the expected low population in both phases and on the absence in the IRMPD spectrum of a diagnostic band predicted at 1667  $\text{cm}^{-1}$  that corresponds to the C–N stretching mode.

Regarding all other higher energy structures considering different G tautomers, reported in Tables SI 1-6, their expected relative populations are very low to be detected and in addition some diagnostic bands are missing in the IRMPD spectrum. Therefore, these structures were neglected and not considered in the present analysis although their existence cannot be completely ruled-out.

In this context, the IRMPD spectrum of the  $[\text{GAg-H}_2\text{O}]^+$  complex can be assigned to a mixture of the  $[\text{GKA}(1,9)\text{N7Ag-H}_2\text{O}]^+$  and  $[\text{GKA}(1,7)\text{N9Ag-H}_2\text{O}]^+$  isomers, although the presence of  $[\text{GKA}(1,7)\text{N3Ag-H}_2\text{O}]^+$  can only be ruled out based on its calculated relative population at 298 K.

The relative intensity of the experimental bands at 1715  $\text{cm}^{-1}$  and 1765  $\text{cm}^{-1}$  ( $I_{1765\text{cm}^{-1}}/I_{1715\text{cm}^{-1}} = 0.65$ ) is related to the relative population of the  $[\text{GKA}(1,7)\text{N9Ag-H}_2\text{O}]^+/\text{GKA}(1,9)\text{N7Ag-H}_2\text{O}]^+$  isomers, which compares better to the estimated Boltzmann R.P. at 298 K in aqueous phase (0.6 with PCM or 0.4 with IFPCM) than in gas phase ( $1 \times 10^{-3}$  at B3LYP or  $4 \times 10^{-4}$  at CCD//B3LYP level). This suggests that the tautomers population in solution is maintained upon vaporization in the ESI source, as previously observed for  $[\text{CGH}]^+$ ,<sup>37</sup>  $[\text{C}_{(-\text{H})}\text{Ba}]^+$ ,<sup>52</sup>  $[\text{CGAg}]^+$ ,<sup>30</sup> complex and  $[\text{Thymidine-Na}]^+$ .<sup>53</sup>

### 3.2. $[\text{GAgG}]^+$ complex

The  $[\text{GAgG}]^+$  complex was isolated in the 7T FT-ICR hybrid mass spectrometer following the procedure described in section 3.1 and further irradiated by 1.0 s with IR-FEL photons. Given the low fragmentation efficiency of this ion, irradiation with a  $\text{CO}_2$  laser during 5.0 ms was necessary to improve the signal to noise ratio, which suggests a higher stability of the  $[\text{GAgG}]^+$  ion towards dissociation as compared to the  $[\text{GAg-H}_2\text{O}]^+$  ion.

The IRMPD process of the  $[\text{GAgG}]^+$  complex leads to the  $[\text{GAg}]^+$  fragment produced as a consequence of the loss of a neutral G. The neutral G loss has been previously identified as the main photofragmentation channel upon UV (266 nm photons) irradiation of the same complex.<sup>24</sup> This single fragmentation channel was considered to obtain the IRMPD spectrum reported in Figure 2a.

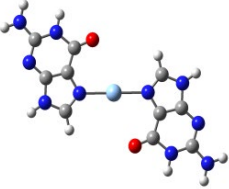
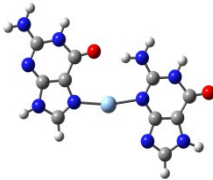
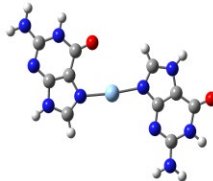
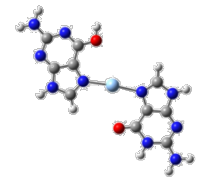
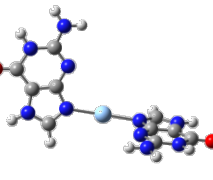
The conformational search for possible isomers of the  $[\text{GAgG}]^+$  complex was based on the results obtained for the  $[\text{GAg-H}_2\text{O}]^+$  complexes in which G was only found in the keto-amino tautomeric forms GKA(1,9) and GKA(1,7). In addition, in neutral G dimers both G moieties were found to be also in their keto-amino forms, although in those experiments the free enol-amino tautomer (GEA(9)) was present in the molecular beam.<sup>54</sup> In this sense, GKA(1,9) and GKA(1,7) were mainly considered to calculate the stability of different isomers of the  $[\text{GAgG}]^+$  complex. Calculations were also performed considering the GEA(9) isomer but in all cases they were less stable than the isomers containing two GKA tautomers, as shown in the Supplementary Information (Table SI9).

The lowest energy structures of the  $[\text{GAgG}]^+$  complex containing GKA(1,9), GKA(1,7) and also the most stable structure containing one GEA(9) molecule are shown in Table 2. From these results, three structures containing GKA tautomers lie very close in energy, hence significant populations of these isomers are expected and all of them can contribute to the IRMPD spectrum.

The global minimum in gas and aqueous phases corresponds to the  $[\text{GKA}(1,9)\text{N7-Ag-N7GKA}(1,9)]^+$  isomer, in which both G moieties are in their GKA(1,9) tautomeric form interacting simultaneously with  $\text{Ag}^+$  through their N7 atoms, leading to a planar structure with the N7- $\text{Ag}^+$ -N7 angle being  $180^\circ$ .

The first local minimum in the gas phase corresponds to the  $[\text{GKA}(1,9)\text{N7-Ag-N3GKA}(1,7)]^+$  isomer that is found at 2.7 kcal/mol above the global minimum. In this isomer  $\text{Ag}^+$  interacts simultaneously through the N7 and N3 atoms of GKA(1,9) and GKA(1,7), respectively. These results are consistent with those previously reported by Cao et al. for the  $[\text{GMG}]^+$  complexes (with  $M = \text{Cu}, \text{Ag}$  and  $\text{Au}$ ).<sup>24</sup> However, they did not report the  $[\text{GKA}(1,9)\text{N7-Ag-N9GKA}(1,7)]^+$  isomer, which according to the results shown in Table 2, is only 2.8 kcal/mol above the global minimum in gas phase and it becomes the first local minimum in aqueous solution being only 1.2 kcal/mol above the global minimum.

**Table 2.** Relative standard Gibbs energies calculated at 298K ( $\Delta G^{\circ}_{298\text{ K}}$ ) for the most stable isomers of the  $[\text{GAgG}]^+$  complex and the relative energies corrected by the effect (PCM). Relative populations (R.P.) of the isomers at 298 K were calculated assuming a Boltzmann distribution.

Structure	Gas phase		PCM (water)	
	$\Delta G^{\circ}_{298\text{ K}}$ (kcal/mol)	R.P. 298 K	$\Delta G^{\circ}_{298\text{ K}}$ (kcal/mol)	R.P. 298 K
	0	1	0	1
[GKA(1,9)N7-Ag-N7GKA(1,9)] <sup>+</sup>				
	2.7	1x10 <sup>-2</sup>	2.2	2x10 <sup>-2</sup>
[GKA(1,9)N7-Ag-N3GKA(1,7)] <sup>+</sup>				
	2.8	1x10 <sup>-2</sup>	1.2	0.1
[GKA(1,9)N7-Ag-N9GKA(1,7)] <sup>+</sup>				
	5.0	2x10 <sup>-4</sup>	8.2	1x10 <sup>-6</sup>
[GKA(1,9) <i>anti</i> N7-Ag-N7GKA(1,9)] <sup>+</sup>				
	5.8	6x10 <sup>-5</sup>	2.4	2x10 <sup>-2</sup>
[GKA(1,7)N9-Ag-N9GKA(1,7)] <sup>+</sup>				

Finally, the  $[\text{GKA}(1,9)_{\text{anti}}\text{N7-Ag-N7GKA}(1,9)]^+$  and  $[\text{GKA}(1,7)\text{N9-Ag-N9GKA}(1,7)]^+$  isomers are higher in energy with a very low predicted population in the gas phase. However, the  $[\text{GKA}(1,7)\text{N9-Ag-N9GKA}(1,7)]^+$  isomer is strongly stabilized by the solvent, and its expected population in aqueous solution is similar to that of the

[GKA(1,9)N7-Ag-N3GKA(1,7)]<sup>+</sup> isomer. Therefore, formation of the [GKA(1,7)N9-Ag-N9GKA(1,7)]<sup>+</sup> isomer cannot be completely ruled-out.

Comparison of the IRMPD spectrum with calculated IR spectra for the five isomers is shown in Figure 2. As observed in Figure 2, the whole IRMPD spectrum could be satisfactorily assigned considering predicted IR transitions for the most stable [GKA(1,9)N7-Ag-N7GKA(1,9)]<sup>+</sup> isomer. However, in the most structurally diagnostic region (1700–1800 cm<sup>-1</sup>) corresponding to the C=O stretching modes two very weak transitions are observed at 1730 cm<sup>-1</sup> and 1750 cm<sup>-1</sup>, which cannot be assigned considering only the most stable isomer.

The C=O stretching modes of the [GKA(1,7)N9-Ag-N9GKA(1,7)]<sup>+</sup> isomer is calculated at 1794 cm<sup>-1</sup> and cannot reproduce any of the experimental bands in the 1700 - 1800 cm<sup>-1</sup> spectral region. As a consequence, the presence of this isomer cannot be confirmed.

Regarding the mixed [GEA(9)<sub>anti</sub>N7-Ag-N7GKA(1,9)]<sup>+</sup> isomer, the calculated C=O stretching mode (1770 cm<sup>-1</sup>) is close to experimental band at 1750 cm<sup>-1</sup>. However, there is no clear signature of the prominent group of bands calculated in the 1650-1720 cm<sup>-1</sup> spectral region. Thus, the existence of this isomer cannot be assured either.

The experimental and calculated C=O stretching frequencies for the three remaining isomers are shown in Table 3. On one hand, the band observed in the IRMPD spectrum at 1750 cm<sup>-1</sup> could be assigned to the C=O stretching mode of both GKA(1,9) in the [GKA(1,9)N7-Ag-N7GKA(1,9)]<sup>+</sup> isomer, calculated at 1747 cm<sup>-1</sup> and/or to the C=O stretching mode of the GKA(1,7) moiety in the [GKA(1,9)N7-Ag-N9GKA(1,7)]<sup>+</sup> isomer, calculated at 1756 cm<sup>-1</sup>. On the other hand, the band observed at 1730 cm<sup>-1</sup> is better assigned to the C=O stretching mode of the GKA(1,9) in the [GKA(1,9)N7-Ag-N9GKA(1,7)]<sup>+</sup> isomer.

**Table 3.** Summary experimental and calculated vibrational frequencies for the two lowest energy isomers of the [GAgG]<sup>+</sup> complex, together with their corresponding assignment.

Exp. (cm <sup>-1</sup> )	Calculated (cm <sup>-1</sup> )		
	[GKA(1,9)N7-Ag N7GKA(1,9)]	[GKA(1,9)N7-Ag N3GKA(1,7)] <sup>+</sup>	[GKA(1,9)N7-Ag N9GKA(1,7)] <sup>+</sup>
1730		1720 (ν <sub>C=O</sub> of GKA(1,9))	1733(ν <sub>C=O</sub> of GKA(1,9))
1750	1747 (ν <sub>C=O</sub> of GKA(1,9))	1770 (ν <sub>C=O</sub> of GKA(1,7))	1756 (ν <sub>C=O</sub> of GKA(1,7))

ν= Stretching

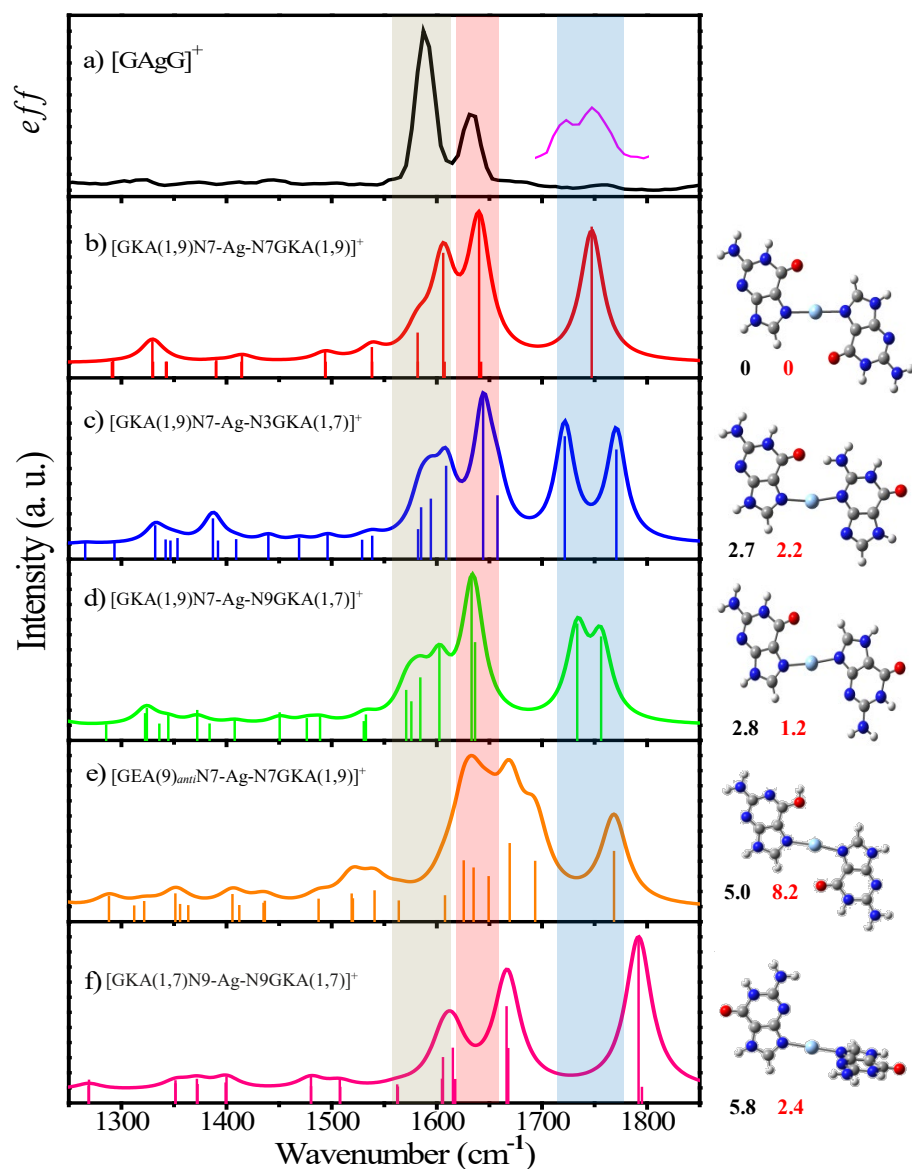


**Figure 2.** a) Experimental IRMPD spectrum of  $[\text{GAgG}]^+$  complex recorded in the spectral range  $1250\text{--}1850\text{ cm}^{-1}$ . The spectrum shown in pink line was recorded between  $1650\text{--}1850\text{ cm}^{-1}$  by irradiation with IR FEL photons for 1 s and 5ms with the  $\text{CO}_2$  laser. Calculated spectra of the three lowest energy isomers at the B3LYP/6-311G++ (d,p) and SDD level for  $\text{Ag}^+$ : b)  $[\text{GKA}(1,9)\text{N7-Ag-N7GKA}(1,9)]^+$ , c)  $[\text{GKA}(1,9)\text{N7-Ag-N3GKA}(1,7)]^+$ , d)  $[\text{GKA}(1,9)\text{N7-Ag-N9GKA}(1,7)]^+$ , e)  $[\text{GEA}(9)_{\text{anti}}\text{N7-Ag-N7GKA}(1,9)]^+$  and f)  $[\text{GKA}(1,7)\text{N9-Ag-N9GKA}(1,7)]^+$ . The vibrational frequencies were corrected with a factor of 0.983. The relative standard Gibbs energies in gas (black numbers) and solution (red numbers) phase are reported in kcal/mol.

The contribution of the  $[\text{GKA}(1,9)\text{N7-Ag-N3GKA}(1,7)]^+$  isomer cannot be neglected considering the present results. However, the energy difference between the two C=O bands experimentally observed is  $20\text{ cm}^{-1}$ , while this difference is  $50\text{ cm}^{-1}$  for the  $[\text{GKA}(1,9)\text{N7-Ag-N3GKA}(1,7)]^+$  isomer and  $23\text{ cm}^{-1}$  for the  $[\text{GKA}(1,9)\text{N7-Ag-N9GKA}(1,7)]^+$  isomer.



N9GKA(1,7)]<sup>+</sup> isomer. Whatever the isomer of the [GAgG]<sup>+</sup> complex is, they are both composed of one GKA(1,9) and one GKA(1,7) moieties.

Therefore, it may be suggested that based on the above discussion of the IRMPD spectrum, a mixture of two or three isomers of [GAgG]<sup>+</sup> complex are formed under our experimental conditions, namely [GKA(1,9)N7-Ag-N7GKA(1,9)]<sup>+</sup> and [GKA(1,9)N7-Ag-N3GKA(1,7)]<sup>+</sup> and/or [GKA(1,9)N7-Ag-N9GKA(1,7)]<sup>+</sup>.

### 3.3. [GAg]<sup>+</sup> complex produced by CID of the [GAgG]<sup>+</sup> complex

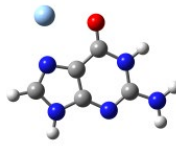
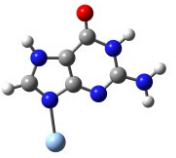
To get more information on the chemical composition (G tautomers identity) of the [GAgG]<sup>+</sup> complex, it was fragmented by Collision Induced Dissociation (CID) in the hexapole trap, and the generated [GAg]<sup>+</sup> fragment was isolated in the FT-ICR cell where it was further explored by IRMPD spectroscopy in the 1250–1850 cm<sup>-1</sup> spectral range.

The fragmentation of the [GAg]<sup>+</sup> fragment by IRMPD leads to the loss of *m/z* 17, probably due to an NH<sub>3</sub> molecule loss as the major channel and loss of a G molecule as a minor channel. Therefore, these two fragmentation channels were considered to obtain the IRMPD spectrum shown in Figure 3a. The structural assignment of the [GAg]<sup>+</sup> complexes is based on the comparison of the IRMPD spectrum with the IR absorption spectra calculated for the possible isomers that can be formed from the interaction between G and Ag<sup>+</sup>.

Since the energy barriers for tautomerization of free G are very high (1.5 – 1.7 eV),<sup>55</sup> this process cannot take place upon CID of the precursor [GAgG]<sup>+</sup> or during the thermalization process of the [GAg]<sup>+</sup> fragment in the hexapole trap. Therefore, we assume that the tautomeric identity of G is maintained as in the precursor [GAgG]<sup>+</sup> ion during these processes. However, the [GAg]<sup>+</sup> fragment could isomerize to a different interaction motif of Ag<sup>+</sup> with G. Therefore, we expect [GKA(1,9)Ag]<sup>+</sup> and/or [GKA(1,7)Ag]<sup>+</sup> fragments, depending on the [GAgG]<sup>+</sup> precursor isomer. Thus, structure and vibrational frequencies of several isomers of these fragments were calculated.

Among the calculated structures, [GKA(1,9)N7Ag]<sup>+</sup> and [GKA(1,7)N9Ag]<sup>+</sup> are the two most stable isomers in gas phase as shown in Table 4, while the [GKA(1,7)N3Ag]<sup>+</sup> isomer evolved spontaneously to the [GKA(1,7)N9Ag]<sup>+</sup> isomer upon optimization. At variance with [GAgG]<sup>+</sup> and [GAg–H<sub>2</sub>O]<sup>+</sup> complexes, in the case of [GAg]<sup>+</sup> the solvent effect was not considered since this ion is not produced in the ESI source but in gas phase within the hexapole trap. Therefore, comparison of the relative stabilities of the [GAg]<sup>+</sup> isomers in solution is meaningless for the interpretation of the present results.

**Table 4.** Relative standard Gibbs free energies calculated at 298K ( $\Delta G^\circ$ ) for the isomers of  $[\text{GAg}]^+$  complex. Relative populations (R.P.) were calculated assuming a Boltzmann distribution, considering that the temperature of the ions is approximately 298 K.

Structure	Gas phase	
	$\Delta G^\circ_{298\text{K}}$ (kcal/mol)	R.P. 298 K
 [GKA(1,9)N7Ag] <sup>+</sup>	0	1
 [GKA(1,7)N9Ag] <sup>+</sup>	8.1	1x10 <sup>-6</sup>

The comparison of the IRMPD spectrum of the  $[\text{GAg}]^+$  complex recorded in the spectral range 1250–1850  $\text{cm}^{-1}$  with the IR spectra calculated for the three most stable isomers is shown in Figure 3. The band at 1635  $\text{cm}^{-1}$  in the IRMPD spectrum is assigned to the bending mode of the  $\text{NH}_2$  group of GKA(1,9) and GKA(1,7) in the  $[\text{GKA}(1,9)\text{N7Ag}]^+$  and  $[\text{GKA}(1,7)\text{N9Ag}]^+$  isomers and calculated at 1642  $\text{cm}^{-1}$  and 1641  $\text{cm}^{-1}$ , respectively.

The bands observed at 1780  $\text{cm}^{-1}$  and at 1590  $\text{cm}^{-1}$  in the IRMPD spectrum are the diagnostic bands for the presence of the  $[\text{GKA}(1,7)\text{N9Ag}]^+$  isomer. These bands are calculated at 1774 and 1590  $\text{cm}^{-1}$  and are assigned to the C=O stretching mode and the N3–C4 stretching mode of GKA(1,7) in the  $[\text{GKA}(1,7)\text{N9Ag}]^+$  isomer, respectively.

The band observed at 1675  $\text{cm}^{-1}$  in the IRMPD spectrum is a diagnostic band for the  $[\text{GKA}(1,9)\text{N7Ag}]^+$  isomer and is assigned to the C=O stretch mode of GKA(1,9), calculated at 1681  $\text{cm}^{-1}$ .

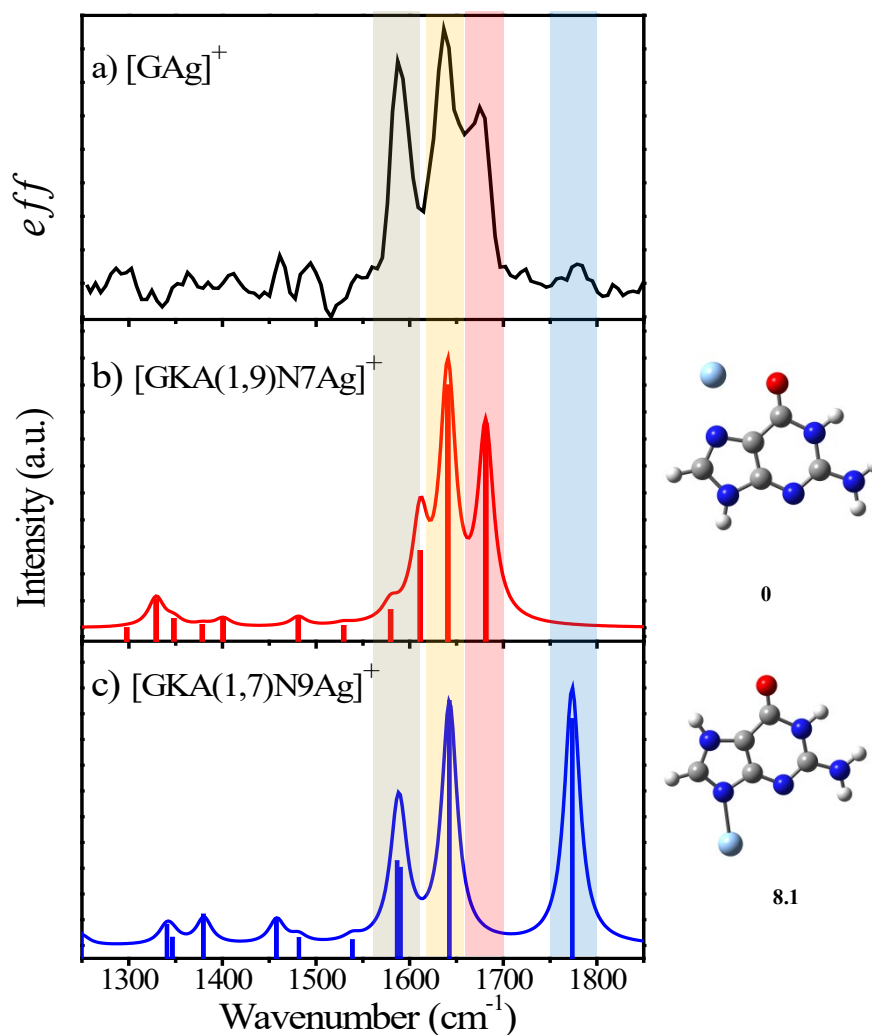


**Figura 3.** a) Experimental IRMPD spectrum of  $[\text{GAg}]^+$  complex recorded in the spectral range  $1250\text{--}1850\text{ cm}^{-1}$  and calculated spectra of the three lowest energy isomers at the B3LYP/6-311G++(d,p) and SDD level for  $\text{Ag}^+$ : b)  $[\text{GKA}(1,9)\text{N7Ag}]^+$  and c)  $[\text{GKA}(1,7)\text{N9Ag}]^+$ . The vibrational frequencies were corrected with a factor of 0.983. The relative standard Gibbs energies in gas phase (black numbers) are reported in kcal/mol.

The C=O stretch mode of GKA(1,9) in the  $[\text{GKA}(1,9)\text{N7Ag}]^+$  isomer, experimentally found at  $1675\text{ cm}^{-1}$  and calculated at  $1681\text{ cm}^{-1}$ , shows a strong redshift as compare to the same vibrational mode in the  $[\text{GKA}(1,9)\text{N7Ag}\text{--}\text{H}_2\text{O}]^+$  and  $[\text{GKA}(1,9)\text{N7AgN7GKA}(1,9)]^+$  isomers calculated at  $1715$  and  $1747\text{ cm}^{-1}$ , respectively. This shift is reasonable since in the  $[\text{GKA}(1,9)\text{N7Ag}]^+$  isomer the  $\text{Ag}^+$  cation bonded to N7 partially interacts with the O atom of the C=O group decreasing the charge density at the C=O bond and stretching its bond distance as shown in Table 5. For the other two complexes the  $\text{dO}\text{--}\text{Ag}^+$  is longer and the C=O stretching mode is barely affected by the interaction with  $\text{Ag}^+$ .

**Table 5:** Selected Bond Lengths of  $[\text{GAg}]^+$ ,  $[\text{GAg-H}_2\text{O}]^+$  and  $[\text{GAgG}]^+$  complexes between Guanine and  $\text{Ag}^+$  (in Å).

Structure	d N7–Ag (Å)	d O–Ag (Å)	d C6–O (Å)
$[\text{GKA}(1,9)\text{N7Ag}]^+$	2.30	2.43	1.24
$[\text{GKA}(1,9)\text{N7Ag-H}_2\text{O}]^+$	2.16	2.86	1.22
$[\text{GKA}(1,9)\text{N7AgN7GKA}(1,9)]^+$	2.14	3.23	1.22

Consequently, the IRMPD spectrum can be completely assigned considering the  $[\text{GKA}(1,9)\text{N7Ag}]^+$  and  $[\text{GKA}(1,7)\text{N9Ag}]^+$  isomers for which diagnostic spectral features were found. The  $[\text{GKA}(1,9)\text{N7Ag}]^+$  fragment can be produced from CID of the  $[\text{GKA}(1,9)\text{N7-Ag-N7GKA}(1,9)]^+$  or the  $[\text{GKA}(1,9)\text{N7-Ag-N9GKA}(1,7)]^+ / [\text{GKA}(1,9)\text{N7-Ag-N3GKA}(1,7)]^+$  isomers, while the  $[\text{GKA}(1,7)\text{N9Ag}]^+$  fragment can be produced from CID of the  $[\text{GKA}(1,9)\text{N7-Ag-N9GKA}(1,7)]^+ / [\text{GKA}(1,9)\text{N7-Ag-N3GKA}(1,7)]^+$  isomer only. Therefore, these results allow confirming the presence of the lesser stable  $[\text{GKA}(1,9)\text{N7-Ag-N9GKA}(1,7)]^+ / [\text{GKA}(1,9)\text{N7-Ag-N3GKA}(1,7)]^+$  isomer of the  $[\text{GAgG}]^+$  complex.

We have been unable to find evidence of the presence of GEA(9) in any of the complexes studied, although this tautomer has been previously found in gas phase<sup>3,4,13,14</sup> and it is almost isoenergetic with the two GKA tautomers found in this work.

There is a general agreement between experimental<sup>3,4,13,14</sup> and theoretical<sup>15,17,55,56</sup> works regarding that GKA(1,9), GKA(1,7) and GEA(9) are the most important and stable tautomers of neutral G in gas phase. However, two set of tautomers (GKA(1,9)/GKA(1,7) or GKA(3,7)/GKA(3,9)/GKA(7,9))<sup>15</sup> have been suggested to be the most stables and populated in aqueous solution, depending on the model and theoretical method used to account for the solvent effect.

From the present results, the isomers experimentally found for the  $[\text{GAg-H}_2\text{O}]^+$  and  $[\text{GAgG}]^+$  complexes contain GKA(1,9) and GKA(1,7) in agreement with previous experimental reports,<sup>21,30</sup> leading in both cases to the most stable structures of the complexes in solution. Although no definitively conclusive, these results strongly suggest that the complexes are produced in solution with the most populated GKA(1,9) and GKA(1,7) tautomers of G in aqueous solution at room temperature and their structure is maintained upon vaporization in the ESI source.

## 4. Conclusions

The interaction between G and  $\text{Ag}^+$  was studied by IRMPD spectroscopy coupled to tandem mass-spectrometry and electronic structure calculations at the DFT level. From these studies it was shown that different isomers of  $[\text{GAg}-\text{H}_2\text{O}]^+$  and  $[\text{GAgG}]^+$  complexes are formed with GKA(1,9) and GKA(1,7) tautomers of G. We were unable to find any evidence of the presence of the GEA(9), GKA(3,7), GKA(3,9) or GKA(7,9). However, the presence of this species cannot be completely ruled out as they could be minor tautomers.

The relative population of the different isomers found for  $[\text{GAg}-\text{H}_2\text{O}]^+$  and  $[\text{GAgG}]^+$  complexes is closer to the predicted population in an aqueous solution at room temperature than to expected population in gas phase, suggesting that the complexes are formed in solution and their structure is maintained during the evaporation process in the ESI source. Therefore, these results allows suggesting that two tautomeric forms of G (GKA(1,9) and GKA(1,7)) mainly coexist in aqueous solution in agreement with the previous theoretical results in the seminal work by C. Colominas et al.<sup>17</sup> and with one of the calculation methods used by M. Hanus et al.<sup>15</sup>

## 5. Supporting Information

Relative electronic energies including zero point energy corrections; relative standard Gibbs energies calculated at 298K calculated at B3LYP/6-311G++ (d,p) with SSD effective core pseudo-potential basis set for Ag; correction of relative standard Gibbs energies considering the effect of the solvent (PCM), relative populations at 298 K for all tautomers and isomers studied in this work; molecular structures and calculated IR spectra of different isomers of  $[\text{GAg}-\text{H}_2\text{O}]^+$ .

## Acknowledgments

This work has been conducted within the International Associated Laboratory LEMIR (CNRS/CONICET) and was supported by CONICET (PUE: 22920160100013CO), FONCyT (PICT2016 - N°0276), SeCyT-UNC, MinCyT-Córdoba (PID-2018) and by the EU Horizon 2020 Program (CALIPSO Plus and EU\_FT-ICR\_MS, under grant numbers 730872 and 731077, respectively). The authors are grateful to the staff members at CLIO for technical support. GAP thanks the Labex PALM (ANR-10-LABX-0039-PALM) for the invited Professor grant in 2019.

## References

- (1) Crick, F.; Watson, J. Molecular Structure of Nucleic Acids: A Structure for Deoxyribose Nucleic Acid. *Nature* **1953**, *171*, 737–738.
- (2) Lowdin P.O. Proton Coupling in DNA and Its Biological Implications. *Rev. Mod. Phys.* **1963**, *35*, 724–732.
- (3) de Vries, M. S. In *Gas-Phase IR Spectroscopy and Structure of Biological Molecules*; Rijs, A.; Oomens, O., Eds.; Springer: Switzerland, 2015; pp 271-297.
- (4) de Vries, M. S. In *Tautomerism: Methods and Theories*; Antonov, L. Ed.; Wiley-VCH, 2014; pp 177-196.
- (5) Nir, E.; Grace, L.; Brauer, B.; de Vries, M. S. REMPI Spectroscopy of Jet-Cooled Guanine. *J. Am. Chem. Soc.* **1999**, *121*, 4896-4897.
- (6) Nir, E.; Janzen, C.; Imhof, P.; Kleinermanns, K.; De Vries, M. S. Guanine Tautomerism Revealed by UV-UV and IR-UV Hole Burning Spectroscopy. *J. Chem. Phys.* **2001**, *115*, 4604–4611.
- (7) Mons, M.; Dimicoli, I.; PiuZZi, F.; Tardivel, B.; Elhanine, M. Tautomerism of the DNA Base Guanine and its Methylated Derivative as Studied by Gas-Phase Infrared and Ultraviolet Spectroscopy. *J. Phys. Chem. A.* **2002**, *106*, 5088-5094.
- (8) Chin, W.; Mons, M.; Dimicoli, I.; PiuZZi, F.; Tardivel, B.; Elhanine, M. Tautomer Contribution's to the Near UV Spectrum of Guanine: Towards a Refined Picture for the Spectroscopy of Purine Molecules. *Eur. Phys. J. D.* **2002**, *20*, 347-355.
- (9) Mons, M.; PiuZZi, F.; Dimicoli, I.; Gorb, L.; Leszczynski, J. Near-UV Resonant Two-Photon Ionization Spectroscopy of Gas Phase Guanine: Evidence for the Observation of Three Rare Tautomers. *J. Phys. Chem. A.* **2006**, *110*, 10921–10924.
- (10) Cerny, J.; Spirko, V.; Mons, M.; Hobza, P.; Nachtigallova, D. Theoretical Study of the Ground and Excited States of 7-Methyl Guanine and 9-Methyl Guanine. Comparison with Experiment. *Phys. Chem. Chem. Phys.* **2006**, *8*, 3059-3065.
- (11) Marian, C. M. The Guanine Tautomer Puzzle: Quantum Chemical Investigation of Ground and Excited States. *J. Phys. Chem. A.* **2007**, *111*, 1545-1553.
- (12) Seefeld, K.; Brause, R.; Haber, T.; Kleinermanns, K. Imino Tautomers of Gas-Phase Guanine from Mid-Infrared Laser Spectroscopy. *J. Phys. Chem. A.* **2007**, *111*, 6217-6221.
- (13) Choi, M. Y.; Miller, R. E. Four Tautomers of Isolated Guanine from Infrared Laser Spectroscopy in Helium Nanodroplets. *J. Am. Chem. Soc.* **2006**, *128*, 7320–7328.
- (14) Alonso, J. L.; Peña, I.; López, J. C.; Vaquero, V. Rotational Spectral Signatures of Four Tautomers of Guanine. *Angew. Chemie.* **2009**, *121*, 6257–6259.
- (15) Hanus, M.; Ryjáček, F.; Kabeláč, M.; Kubař, T.; Bogdan, T. V.; Trygubenko, S. A.;

- Hobza, P. Correlated Ab Initio Study of Nucleic Acid Bases and Their Tautomers in the Gas Phase, in a Microhydrated Environment and in Aqueous Solution. Guanine: Surprising Stabilization of Rare Tautomers in Aqueous Solution. *J. Am. Chem. Soc.* **2003**, *125*, 7678–7688.
- (16) Štoček, J. R.; Dračinský, M. Tautomerism of Guanine Analogues. *Biomolecules*. **2020**, *10*, 170.
- (17) Colominas, C.; Luque, F. J.; Orozco, M. Tautomerism and Protonation of Guanine and Cytosine. Implications in the Formation of Hydrogen-Bonded Complexes. *J. Am. Chem. Soc.* **1996**, *118*, 6811–6821.
- (18) Miertuš, S.; Scrocco, E.; Tomasi, J. Electrostatic Interaction of a Solute with a Continuum. A Direct Utilizaion of AB Initio Molecular Potentials for the Prevision of Solvent Effects. *Chem. Phys.* **1981**, *55*, 117–129..
- (19) Miertuš, S.; Tomasi, J. Approximate Evaluations of the Electrostatic Free Energy and Internal Energy Changes in Solution Processes. *Chem. Phys.* **1982**, *65*, 239–245.
- (20) Jorgensen, W. L.; Tirado-Rives, J. Molecular Modeling of Organic and Biomolecular Systems Using BOSS and MCPRO. *J. Comput. Chem.* **2005**, *26*, 1689–1700.
- (21) Berdakin, M.; Féraud, G.; Dedonder-Lardeux, C.; Jouvét, C.; Pino, G. A. Excited States of Protonated DNA/RNA Bases. *Phys. Chem. Chem. Phys.* **2014**, *16*, 10643–10650.
- (22) Gabelica, V.; Rosu, F.; De Pauw, E.; Lemaire, J.; Gillet, J. C.; Pouilly, J. C.; Lecomte, F.; Grégoire, G.; Schermann, J. P.; Desfrancois, C. Infrared Signature of DNA G-Quadruplexes in the Gas Phase. *J. Am. Chem. Soc.* **2008**, *130*, 1810–1811.
- (23) Chiavarino, B.; Crestoni, M. E.; Fornarini, S.; Scuderi, D.; Salpin, J. Y. Interaction of Cisplatin with Adenine and Guanine: A Combined IRMPD, MS/MS, and Theoretical Study. *J. Am. Chem. Soc.* **2013**, *135*, 1445–1455.
- (24) Cao, G. J.; Xu, H. G.; Xu, X. L.; Wang, P.; Zheng, W. J. Photodissociation and Density Functional Calculations of  $A_2M^+$  and  $G_2M^+$  (A = Adenine, G = Guanine, M = Cu, Ag, and Au) Cluster Ions. *Int. J. Mass Spectrom.* **2016**, *407*, 118–125.
- (25) Russo, N.; Toscano, M.; Grand, A. Bond Energies and Attachments Sites of Sodium and Potassium Cations to DNA and RNA Nucleic Acid Bases in the Gas Phase. *J. Am. Chem. Soc.* **2001**, *123*, 10272–10279..
- (26) Šponer, J.; Sabat, M.; Gorb, L.; Leszczynski, J.; Lippert, B.; Hobza, P. The Effect of Metal Binding to the N7 Site of Purine Nucleotides on Their Structure, Energy, and Involvement in Base Pairing. *J. Phys. Chem. B.* **2000**, *104*, 7535–7544.
- (27) Burda, J. V.; Šponer, J.; Hobza, P. Ab Initio Study of the Interaction of Guanine

and Adenine with Various Mono- and Bivalent Metal Cations ( $\text{Li}^+$ ,  $\text{Na}^+$ ,  $\text{K}^+$ ,  $\text{Rb}^+$ ,  $\text{Cs}^+$ ;  $\text{Cu}^+$ ,  $\text{Ag}^+$ ,  $\text{Au}^+$ ;  $\text{Mg}^{2+}$ ,  $\text{Ca}^{2+}$ ,  $\text{Sr}^{2+}$ ,  $\text{Ba}^{2+}$ ;  $\text{Zn}^{2+}$ ,  $\text{Cd}^{2+}$ , and  $\text{Hg}^{2+}$ ). *J. Phys. Chem.* **1996**, *100*, 7250–7255.

(28) Azargun, M.; Meister, P. J.; Gault, J. W.; Fridgen, T. D. The  $\text{K}_2(9\text{-Ethylguanine}_{12})^{2+}$  Quadruplex Is More Stable to Unimolecular Dissociation than the  $\text{K}(9\text{-Ethylguanine}_8)^+$  Quadruplex in the Gas Phase: A BIRD, Energy Resolved SORI-CID, IRMPD Spectroscopic, and Computational Study. *Phys. Chem. Chem. Phys.* **2019**, *21*, 15319–15326.

(29) Azargun, M.; Jami-Alahmadi, J.; Fridgen, T. D. The Intrinsic Stabilities and Structures of Alkali Metal Cationized Guanine Quadruplexes. *Phys. Chem. Chem. Phys.* **2017**, *19*, 1281–1287.

(30) Cruz-Ortiz, A. F.; Jara-Toro, R. A.; Berdakin, M.; Loire, E.; Pino, G. A. Gas phase structure and fragmentation of  $[\text{Cytosine-Guanine}]\text{Ag}^+$  complex studied by mass-resolved IRMPD spectroscopy. *Eur. Phys. J. D.* **2021**, *75*, 119-130.

(31) Salpin, J. Y.; Guillaumont, S.; Tortajada, J.; MacAleese, L.; Lemaire, J.; Maitre, P. Infrared Spectra of Protonated Uracil, Thymine and Cytosine. *ChemPhysChem.* **2007**, *8*, 2235–2244.

(32) Yang, B.; Wu, R. R.; Polfer, N. C.; Berden, G.; Oomens, J.; Rodgers, M. T. IRMPD Action Spectroscopy of Alkali Metal Cation-Cytosine Complexes: Effects of Alkali Metal Cation Size on Gas Phase Conformation. *J. Am. Soc. Mass Spectrom.* **2013**, *24*, 1523–1533.

(33) Berdakin, M.; Steinmetz, V.; Maitre, P.; Pino, G. A. On the  $\text{Ag}^+$ -Cytosine Interaction: The Effect of Microhydration Probed by IR Optical Spectroscopy and Density Functional Theory. *Phys. Chem. Chem. Phys.* **2015**, *17*, 25915–.

(34) Taccone, M. I.; Cruz-Ortiz, A. F.; Dezalay, J.; Soorkia, S.; Broquier, M.; Grégoire, G.; Sánchez, C. G.; Pino, G. A. UV Photofragmentation of Cold Cytosine- $\text{M}^+$  Complexes ( $\text{M}^+$ :  $\text{Na}^+$ ,  $\text{K}^+$ ,  $\text{Ag}^+$ ). *J. Phys. Chem. A.* **2019**, *123*, 7744–7750.

(35) Berdakin, M.; Steinmetz, V.; Maitre, P.; Pino, G. A. Gas Phase Structure of Metal Mediated  $(\text{Cytosine})_2\text{Ag}^+$  Mimics the Hemiprotonated  $(\text{Cytosine})_2\text{H}^+$  Dimer in  $i$ -Motif Folding. *J. Phys. Chem. A.* **2014**, *118*, 3804–3809.

(36) Géraldine Féraud; Berdakin, M.; Dedonder, C.; Jouvét, C.; Pino, G. A. Excited States of Proton-Bound DNA / RNA Base Homodimers : Pyrimidines. *J. Phys. Chem. B.* **2015**, *119*, 2219–2228.

(37) Cruz-Ortiz, A. F.; Rossa, M.; Berthias, F.; Berdakin, M.; Maitre, P.; Pino, G. A. Fingerprints of Both Watson-Crick and Hoogsteen Isomers of the Isolated (Cytosine-



Guanine) $H^+$  Pair. *J. Phys. Chem. Lett.* **2017**, *8*, 5501–5506.

(38) Bakker, J. M.; Besson, T.; Lemaire, J.; Scuderi, D.; Maitre, P. Gas-Phase Structure of a  $\pi$ -Allyl-Palladium Complex: Efficient Infrared Spectroscopy in a 7 T Fourier Transform Mass Spectrometer. *J. Phys. Chem. A* **2007**, *111*, 13415–13424.

(39) Donald, W. A.; Khairallah, G. N.; O’Hair, R. A. J. The Effective Temperature of Ions Stored in a Linear Quadrupole Ion Trap Mass Spectrometer. *J. Am. Soc. Mass Spectrom.* **2013**, *24*, 811–815.

(40) Prazeres, R.; Glotin, F.; Insa, C.; Jaroszynski, D. A.; Ortega, J. M. Two-Colour Operation of a Free-Electron Laser and Applications in the Mid-Infrared. *Eur. Phys. J. D* **1998**, *3*, 87–93.

(41) Sinha, R. K.; Nicol, E.; Steinmetz, V.; Maitre, P. Gas Phase Structure of Micro-Hydrated  $[Mn(ClO_4)]^+$  and  $[Mn_2(ClO_4)_3]^+$  Ions Probed by Infrared Spectroscopy. *J. Am. Soc. Mass Spectrom.* **2010**, *21*, 758–772.

(42) Frisch, M. J.; Trucks, G. W.; Schlegel, H. B.; Scuseria, G. E.; Robb, M. A.; Cheeseman, J. R.; Scalmani, G.; Barone, V.; Mennucci, B.; Petersson, G. A.; Gaussian 09, revision E.01; Gaussian Inc.: Wallingford, CT, 2009.

(43) Becke, A. D. Density-Functional Thermochemistry. III. The Role of Exact Exchange. *J. Chem. Phys.* **1993**, *98*, 5648–5652.

(44) Lee, C.; Yang, W.; Parr, R. C. Development of the Colle-Salvetti correlation-energy formula into a functional of the electron density. *Phys. Rev. B* **1988**, *37*, 785–789.

(45) Andrae, D.; Häußermann, U.; Dolg, M.; Stoll, H.; Preuß, H. Energy-Adjusted Ab Initio Pseudopotentials for the Second and Third Row Transition Elements. *Theor. Chim. Acta* **1990**, *77*, 123–141.

(46) Riley, K. E.; Op’t Holt, B. T.; Merz, K. M. Jr. Critical Assessment of the Performance of Density Functional Methods for Several Atomic and Molecular Properties. *J. Chem. Theory Comput.* **2007**, *3*, 407-433.

(47) Tirado-Rives, J.; Jorgensen, W. L. Performance of B3LYP Density Functional Methods for a Large Set of Organic Molecules. *J. Chem. Theory Comput.* **2008**, *4*, 297-306.

(48) Halls, M. D.; Velkovski, J.; Schlegel, H. B. Harmonic Frequency Scaling Factors for Hartree-Fock, S-VWN, B-LYP, B3-LYP, B3-PW91 and MP2 with the Sadlej PVTZ Electric Property Basis Set. *Theor. Chem. Acc.* **2001**, *105*, 413–421.

(49) Tomasi, J.; Mennucci, B.; Cammi, R. Quantum Mechanical Continuum Solvation Models. *Chem. Rev.* **2005**, *105*, 2999–3093.

- (50) Klamt, A.; Moya, C.; Palomar, J. A Comprehensive Comparison of the IEFPCM and SS(V)PE Continuum Solvation Methods with the COSMO Approach. *J. Chem. Theory Comput.* **2015**, *11*, 4220–4225.
- (51) Martínez, A. Theoretical Study of Guanine-Cu and Uracil-Cu (Neutral, Anionic, and Cationic). Is It Possible to Carry out a Photoelectron Spectroscopy Experiment? *J. Chem. Phys.* **2005**, *123*, 024311(1- 8).
- (52) Cruz-Ortiz, A. F.; Taccone, M. I.; Maitre, P.; Rossa, M.; Pino, G. A. On the Interaction Between Deprotonated Cytosine (C<sub>-H</sub>) and Ba<sup>2+</sup>: Infrared Multiphoton Spectroscopy and Dynamics. *ChemPhysChem.* **2020**, *21*, 2571-2582
- (53) Zhu, Y.; Roy, H. A.; Cunningham, N. A.; Strobehn, S. F.; Gao, J.; Munshi, M. U.; Berden, G.; Oomens, J.; Rodgers, M. T. IRMPD Action Spectroscopy, ER-CID Experiments, and Theoretical Studies of Sodium Cationized Thymidine and 5-Methyluridine : Kinetic Trapping During the ESI Desolvation Process Preserves the Solution Structure. *J. Am. Soc. Mass Spectrom.* **2017**, *28*, 2423–2437.
- (54) Nir, E.; Janzen, C.; Imhof, P.; Kleinermanns, K.; de Vries, M. S. Pairing of the Nucleobase Guanine Studied by IR–UV Double-Resonance Spectroscopy and Ab-Initio Calculations. *Phys. Chem. Chem. Phys.* **2002**, *4*, 740–750.
- (55) Leszczynski, J. The Potential Energy Surface of Guanine Is Not Flat : An Ab Initio Study with Large Basis Sets and Higher Order Electron Correlation Contributions. *J. Phys. Chem. A.* **1998**, *102*, 2357–2362.
- (56) Shukla, M. K.; Leszczynski, J. Tautomerism in Nucleic Acid Bases and Base Pairs: A Brief Overview. *WIREs: Comput. Mol. Sci.* **2013**, *3*, 637-649.